Endocrine (2019) 63:615–631
https://doi.org/10.1007/s12020-018-1810-2

ORIGINAL ARTICLE

Inactivation of the Ras/MAPK/PPARγ signaling axis alleviates diabetic mellitus-induced erectile dysfunction through suppression of corpus cavernosal endothelial cell apoptosis by inhibiting HMGCS2 expression

Zhuo Zhang[1] · Hai-Yan Zhang[2] · Ying Zhang[3] · Hai Li[1]

Received: 23 May 2018 / Accepted: 30 October 2018 / Published online: 20 November 2018

Abstract

Purpose Diabetic mellitus-induced erectile dysfunction (DMED) represents a significant complication associated with diabetes mellitus (DM) that greatly affects human life quality. Various reports have highlighted the involvement of mitochondrial 3-hydroxy-3-methylglutaryl-CoA synthase 2 (HMGCS2) in the regulation of mitochondrial fatty acid oxidation, which has also been linked with DM. Through bioinformatics analysis, HMGCS2 was determined to be a novel target among DM patients suffering from erectile dysfunction (ED), and enriched in the Ras/ERK/PPAR signaling axis. Owing to the fact that the key mechanism HMGCS2 involved in DM remains largely unknown, we set out to investigate the role of the Ras/MAPK/PPARγ signaling axis and HMGCS2 in the corpus cavernosal endothelial cells (CCECs) of rats with DMED.

Methods Firstly, bioinformatics analysis was used to screen out differentially expressed genes in DMED. Then, to investigate the influence of the Ras/MAPK/PPARγ signaling axis and HMGCS2 on DMED, a rat model of DMED was established and injected with Simvastatin and si-Hmgcs2. The individual expression patterns of Ras, MAPK, PPARγ and HMGCS2 were determined by RT-qPCR, immunohistochemistry and western blot analysis methods. Afterwards, to investigate the mechanism of Ras/MAPK/PPARγ signaling axis and HMGCS2, CCECs were isolated from DMED rats and transfected with agonists and inhibitors of the Ras/MAPK/PPARγ signaling axis and siRNA of HMGCS2, with their respective functions in apoptosis and impairment of CCECs evaluated using TUNEL staining and flow cytometry.

Results Microarray analysis and KEGG pathway enrichment analysis revealed that Ras/ERK/PPAR signaling axis mediated HMGCS2 in DMED. Among the DMED rats, the Ras/MAPK/PPAR signaling axis was also activated while the expression of HMGCS2 was upregulated. The activation of Ras was determined to be capable of upregulating ERK expression which resulted in the inhibition of the transcription of PPARγ and subsequent upregulation of HMGCS2 expression. The inhibited activation of the Ras/ERK/PPAR signaling axis and silencing HMGCS2 were observed to provide an alleviatory effect on the injury of DMED while acting to inhibit the apoptosis of CCECs.

Conclusion Collectively, the key findings suggested that suppression of the Ras/MAPK/PPARγ signaling axis could downregulate expression of HMGCS2, so as to alleviate DMED. This study defines the potential treatment for DMED through inhibition of the Ras/MAPK/PPARγ signaling axis and silencing HMGCS2.

Keywords Diabetic mellitus-induced erectile dysfunction · Corpus cavernosal endothelial cells · Mitochondrial 3-hydroxy-3-methylglutaryl-CoA synthase 2 · Ras/MAPK/PPARγ signaling axis · Apoptosis

These authors contributed equally: Zhuo Zhang, Hai-Yan Zhang.

✉ Hai Li
lihai@jlu.edu.cn

[1] Department of Urology, China-Japan Union Hospital of Jilin University, 130000 Changchun, P.R. China

[2] Department of Gastrointestinal Surgery, China-Japan Union Hospital of Jilin University, 130000 Changchun, P.R. China

[3] Department of Pathology, China-Japan Union Hospital of Jilin University, 130000 Changchun, P.R. China

Introduction

Erectile dysfunction (ED) is defined as impotency in men, relating to the distinctive inability to acquire or sustain sufficient erectile function required for satisfaction during sexual intercourse [1]. ED primarily affects men over the age of 40 years old, with statistics predicting that approximately 322 million males would suffer from ED worldwide by the year 2025 [2]. A consensus exits regarding the association between diabetes mellitus (DM) and sexual dysfunction, dating all the way back to the tenth century when Avicenna suggested the "collapse of sexual function" as a specific complication associated with DM [3]. As one of the chief complications of DM, ED has been indicated to affect approximately 50% of male patients with DM within 10 years of their diagnosis [4]. Cavernous endothelium plays a significant role in regulating underlying smooth muscle tone and physiological penile erection, which contributes to cavernosal smooth muscle cell relaxation allowing the initiation and maintenance of erectile function [5]. Furthermore, endothelial dysfunction has been indicated to be a consequence of certain harmful events including high glucose levels, enhanced arginase activity as well as enhanced oxidative stress on endothelial cells [6, 7].

Mitochondrial 3-hydroxy-3-methylglutaryl-CoA synthase 2 (HMGCS2), the factor tasked with catalyzing the primary procedure of ketogenesis, plays a crucial role in a large array of metabolic conditions, while the mRNA expression and protein level of HMGCS2 have been suggested to display marked increases with insulin absence in the event of a higher dose of fatty acids or glucose [8]. This being said, deficient HMGCS2 induces episodes of serious hypoglycemia, enhances fatty acid and even leads to metabolic acidosis in fasting states [9]. Peroxisome proliferators-activated receptor gamma (PPARγ) is one of three isoforms compromised by a superfamily of nuclear hormone receptors of PPARs [10]. PPARγ defective or deficient PPARγ could well play a role in the metabolic syndrome caused by fat loss or redistribution as well as in insulin sensitivity [11, 12]. Mitogen-activated protein kinases (MAPK) signaling axis participates in various biological functions including proliferation, transformation and apoptosis, and MAPK can be activated in high glucose [13]. Moreover, the activation of p38 MAPK has been shown to elevate arginase expression/activity in diabetic and hypertensive mice [6]. Pancreatic islet renin-angiotensin system (Ras) activation has been linked to enhanced oxidative stress and impaired insulin secretion [14]. Ras/MAPK inhibitors act as scaffold proteins that aid in regulating PPARγ expression resulting in the inhibition of gastric epithelial cell proliferation [15].

Current existing literature has predominately investigated the relationship between one or two of the components of Ras/MAPK/PPARγ and diabetic mellitus-induced erectile dysfunction (DMED). Since there are limited studies correlating the Ras/MAPK/PPARγ signaling axis and HMGCS2 with DMED, the primary aim of the current study was to investigate the mechanism of DMED in corpus cavernosal endothelial cells (CECCs) in an attempt to identify a novel treatment strategy for DEMD patients.

Materials and methods

Bioinformatics

GEO (https://www.ncbi.nlm.nih.gov/geo/) is a public database store of functional gene; initially we searched the database for related gene expressed in DMED using the key word "diabetes mellitus-induced erectile dysfunction". We found a GSE2457 data set recording the expression of corpus cavernosa in streptomycin-induced in both DM and normal rats. The annotation platform of chip was GPL341-[RAE230A] Affymetrix Rat Expression 230A Array. The chip expression data underwent standardization pretreatment and screening of differentially expressed genes using the limma package of R language [16]. The difference of gene expression imaging was presented with the screening threshold value set from P value < 0.05 to |LogFoldChange| > 2. Finally, the differentially expressed genes underwent KEGG pathway analysis using the String database (https://string-db.org/).

Model establishment of DMED

Ninety male Sprague-Dawley (SD) rats (weight, 270–310 g) were purchased from Shanghai Institute of Pharmaceutical Industry (Shanghai, China), and were housed in a laminar flow cabinet under specific pathogen-free conditions with constant controlled temperature (24–26 °C), and humidity (45–55%). Food and drinking water were sterilized by high temperature. Ten rats were utilized for tissue and cell experiments, while the remaining rats were used for the animal experiment. Mating experimentation was performed in order to assess erectile function.

Next, a total of 80 SD rats were randomly grouped into control and Streptozotocin (STZ) groups and fasted for 16 h. Phosphate buffer saline (PBS) and 60 mg/kg STZ (l% concentration) were injected intraperitoneally in a respective manner into the rats in the control and DMED groups to measure the blood sugar level (BSL) of the rats. In the event that the BSL of the fasting rats was higher than 16.7 mmol/L, the rat was subsequently confirmed diabetic [17]. Eight weeks later, the rats were weighed, with an apomorphine (APO)-induced erection employed in order to select the

DMED rats. The rat subcutaneous neck region was administered with a one-off injection with 100 μg/kg of APO (concentration, 50 μg/mL). Hyperemia of the penis head or growth of the penis was considered to be reflective of an erection in a simultaneous fashion; the existence, number, incubation period, and positive rate of erections were recorded accordingly. DMED rats were considered to be those that failed to exhibit an erection [18]. The rat experiment was divided into two parts. The first part was conducted in order to examine the difference in relation to the expression of Ras, extracellular signal-regulated kinase (ERK), PPARγ and HMGCS2 in corpus cavernosa of DMED rats, and the structure change of corpus cavernosa, as well as the impairment of CCECs. Ten normal rats were assigned into the control group while another ten rats with DMED were placed into the DMED group. The remaining 32 rats were recruited to investigate the effects of the Ras/MAPK/PPARγ signaling pathway and HMGCS2 on DMED. A total of 32 rats confirmed to have DMED were assigned into four groups with eight rats per group as follows: siRNA-negative control (NC) group (corpus cavernosa injected with NC siRNA), Simvastatin (an inhibitor of Ras) group (corpus cavernosa injected with NC siRNA and intragastrically administered with 1 mg/kg Simvastatin) (Merck, NJ, USA), si-HMGCS2 group (corpus cavernosa injected with HMGCS2 interfered siRNA), and Simvastatin + si-Hmgcs2 group (corpus cavernosa injected with HMGCS2-interfered siRNA and intragastrically administered with 1 mg/kg Simvastatin).

Intracavernous pressure (ICP) examination

One percent pentobarbital at 6 mL/kg was injected intraperitoneally into the rats for anesthesia purposes. Next, the corpus cavernosa was separated, with the prostate exposed under the guidance of a surgical microscope. The corpus cavernosa nerve was subsequently located between the posterolateral and the rectum of the prostate, followed by exposure and separation of left common carotid artery. Intracavernous pressure (ICP) and mean artery pressure (MAP) were continually monitored. The electrode stimulation parameters employed were as follows: 20 Hz of frequency, 5 V of electric tension, 0.2 ms of pulse width, and 50 s of stimulus time. The interval of two successive electric stimulations was 15 min. The changes of MAP and ICP in each group were recorded. The rats who failed either the operation or ICP test were excluded from our analysis.

Transmission electron microscopy

The fresh rat corpus cavernosum tissue specimen was prefixed with 3% glutaraldehyde for 12 h, fixed with 1% osmium tetroxide at 4 °C for 2 h, and then dehydrated using 30, 50 and 70% acetone at room temperature for 5–10 min, 90% acetone at room temperature for another 10–15 min, and 100% acetone at room temperature for 40 min (the acetone was changed for three times). The specimen was then immersed with a mixture of Epon8l2 and acetone (a ratio at 3:1) at 35 °C for 45 min, and then immersed in Epon8l2 at 45 °C for 2 h. Afterwards, the specimen was sliced into semi-thin sections (1–2 μm), positioned by optics, and then sliced into ultrathin sections (50–70 nm). After co-staining with uranyl acetate and lead citrate, the ultrastructure of tissue of corpus cavernosum was observed under a transmission electron microscope (TEM, H-600IV, Hitachi, Japan).

Immunohistochemistry

The sliced sections of paraffin-embedded corpus cavernosa were incubated at 60 °C for 1 h, dewaxed in Xylene I and Xylene II respectively for 30 min, and then dehydrated with gradient alcohol. Next, the sections were placed into a diluted potassium citrate solution for antigen retrieval using a microwave oven for heating purposes at 90 °C over a 10-min period, and then cooled down at room temperature. After three PBS washes (5 min each time), the sections were added with 3% H_2O_2 to inactivate endogenous peroxidase, and then blocked with 5% goat serum (Solarbio Science and Technology Co., Ltd., Beijing, China) at room temperature for 20 min. After the sealing fluid was aspirated, anti-mouse Ras monoclonal antibody (ab16907, 1:200), anti-rabbit ERK polyclonal antibody (ab17942, 1:200), anti-rabbit PPARγ polyclonal antibody (ab209350, 1:200) and anti-rabbit HMGCS2 monoclonal antibody (ab137043, 1:500) were subsequently added to the sections in order to completely cover the sections and incubate at 4 °C overnight. All the aforementioned antibodies were procured from Abcam Inc (Cambridge, MA, USA). After three PBS washes (5 min each), the sections were incubated with secondary antibody liquid of goat anti-rabbit or anti-mouse (ZSGB-BIO, Beijing, China) at 37 °C for 1 h, and then washed again with PBS (three times, 5 min each time). The sections were then subsequently colored with (3,3-diaminobenzidine tetrahydrochloride) DAB (ZSGB-BIO, Beijing, China) for 3–5 min, and then fully washed under running water. Cell image analysis was conducted by color cytophotometry (Media Cybernetics Inc., Rockville, MD, USA). Four sections were obtained from each specimen, and three fields were randomly selected in order to determine the positive cell ratio under a light microscope. Lastly, the mean value was calculated to reflect the expression of Ras, ERK, PPARγ, and HMGCS2.

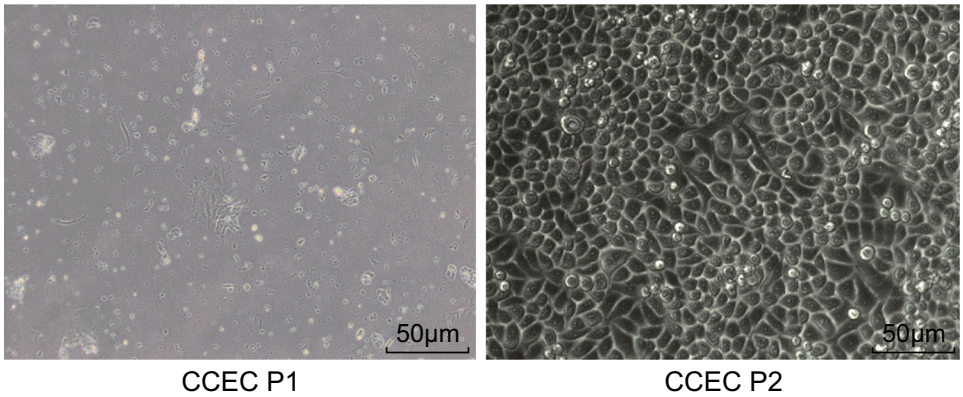

Fig. 1 Cell morphology of rat CCEC P1 and P2 (×200). CCECs corpus cavernosal endothelial cells

Terminal deoxyribonucleotidyl transferse (TdT)-mediated biotin-16-dUTP nick-end labeling (TUNEL) staining

TUNEL kit (Beyotime Biotechnology Co., Ltd., Shanghai, China) was used to detect CCEC apoptosis in corpus cavernosum tissues of the rat. The sliced sections of the paraffin-embedded corpus cavernosum tissues were dewaxed with xylene, hydrated with gradient alcohol, and then immersed in 3% H_2O_2 solution, for 10 min. After 5 min of PBS washing, the sections were treated with 50 μL proteinase K (20 μg/mL) (Sigma-Aldrich, St. Louis, MO, USA). After tissue protein removal at room temperature for 20 min, the sections were washed again with PBS three times (5 min each), followed by the application of antigen retrieval for 30 min with the addition of citrate, with two additional PBS washes performed (5 min each), and reaction with 50 μL TdT enzyme reaction solution at 37 °C for 1 h. The reaction solution without TdT enzyme was regarded as the NC. The sections were then washed with PBS three times (5 min each), reacted with 50 μL peroxidase-labeled anti-digoxigenin at 37 °C for 30 min under conditions void of light, and then washed again with PBS three times (5 min each). The sections were then subsequently stained with DAB (ZSGB-BIO, Beijing, China) for 10 min, rinsed three times with PBS, counterstained with hematoxylin, observed and photographed under a microscope (Nikon, Tokyo, Japan). Five fields were randomly selected in order to determine the number of the normal cells and the positive cells followed by calculation of the cell apoptosis rate (the average number of positive nucleus/the number of all nucleus × 100%).

Isolation of rat CCECs

SD rats were intraperitoneally injected with 3% pentobarbital sodium (30 mg/kg). The penis was then swiftly removed and placed into a fresh PBS solution. Next, the corpus cavernosum was separated, and the cavernous tissue was cleaned and cut into 1–3 mm^3, followed by centrifugation and three PBS washes. After that, the tissues were transferred to a 25 cm^2 culture bottle and treated with 0.025% trypsin I for 60 min. The CCECs were separated by shaking means under a constant controlled temperature of 37 °C. The CCECs were then added with Dulbecco's modified eagle's medium (DMEM) supplemented with 10% fetal bovine serum (FBS) and centrifuged at 112 × *g* for 5 min to remove the supernatant. Afterwards, the digestive suspension was strained using a 400-μm cell strainer in order to separate the undigested tissue, followed by centrifugation at1000 × *g* for 5 min. The supernatant was then discarded with the isolated cells then added to 10% FBS culture medium. The cells were tallied using a blood cell analyzer, with the cell density then adjusted to 1×10^5 cells/mL. The cells were then inoculated into a culture dish and incubated at 37 °C, and with 5% CO_2. The medium was replaced at regular 2-day intervals [7]. Isolated primary cells from CCECs fused into a single cell layer and presented in a cobblestone shape, with a cell doubling time of 72–96 h. After a 7-day period of incubation, the primary cells were subcultured. After 1 h of subculture, cell adherence was analyzed, with the subcultured cells observed to have grown at a rapid rate [7]. CCEC P1 and P2 are depicted in Fig. 1.

Cell treatment and transfection

The Ras signaling axis inhibitor farnesylthiosalicylic acid (FTS) (162520-00-5, Cayman Chemical Company, Ann Arbor, MI, USA) was used for 24-h cell incubation (final concentration: 10 μM). Next, the cells were incubated with Ras signaling axis agonist transforming growth factor α (TGF-α, 100-16A, Peprotech, Rocky Hill, NJ, USA) for 24 h (final concentration: 10 ng/mL), and then MAPK signaling axis agonist C6-Ceramide (sc-217814, Santa Cruz Biotechnology, Santa Cruz, CA, USA) for 24 h (final concentration: 50 μM). Then the cells were cultured with

MAPK signaling axis inhibitor FR180204 (Selleckchem, Houston, TX, USA) [19] for 24 h (final concentration: 50 μM), with PPARγ agonist Rosiglitazone (RGZ, Alexis Biochemicals, San Diego, CA, USA) for 24 h (final concentration: 10 μM) and finally with PPARγ signaling axis inhibitor GW9662 (BML-GR234-0050, Alexis Biochemicals, San Diego, CA, USA) [20] for 24 h (final concentration: 1 μM).

The full-length sequences of Hmgcs2 (forward sequence: 5′-CAGTTCTCGAGTTAATGATGATGATGATGGACGGGACGCCGGGCATACTTTCG-3′; reverse sequence: 5′-ATCCTCTAGAAATAATTTTGTTTAACTTTAAGAAGGAGATATACCATGACAGCCTCTGCTGTCCCCCTGGC-3′) were designed and amplified by means of regular polymerase chain reaction (PCR) and inserted into the plasmid [21]. Plasmid pcDNA™3.1 with ampicillin resistance (Promega corporation, Madison, WI, USA) was synthesized by Shanghai Genechem Co., Ltd (Shanghai, China). Hmgcs2 siRNA and blank control siRNA were purchased from Santa Cruz Biotechnology, Santa Cruz, CA, USA. Transfection reagent (Lipofectamine 2000, Invitrogen Inc., Carlsbad, CA, USA) was conducted for the transfer of plasmid and siRNA sequences into CCECs. One day prior to transfection, the CCECs were inoculated into a six-well plate, and cultured with DMEM containing 10% FBS in a 37 °C incubator with 5% CO_2. The cells were transfected when cell density was observed to have reached 80%. Meanwhile, the compound of Lipofectamine™ 2000 with siRNA or plasmid for each group was prepared respectively in accordance with the instructions of the Lipofectamine 2000 kit. The obtained compound was then added into a six-well plate containing the cells and culture solution, and then slightly shaken to ensure full mixing. The cells were then incubated in 5% CO_2 at 37 °C. After 4 h of transfection, each well was added with 1 mL DMEM containing 10% FBS or high glucose medium (Gibco, Gaithersburg, MD, USA) for further incubation. After 48-h transfection, the cells were collected for subsequent experiments [22].

Reverse transcription quantitative polymerase chain reaction (RT-qPCR)

The total RNA of the CCECs as well as the penis tissues obtained from each group was extracted using the Trizol method (Invitrogen, Carlsbad, CA, USA). The RNA concentration was determined using a Nanodrop 2000 (Thermo Fisher Scientific, San Jose, CA, USA). Next, 1 μg of total RNA was reversely transcribed into cDNA with any contaminated DNA removed using 5× gDNA Eraser Buffer and gDNA Eraser at 42 °C for 2 min according to the instructions of PrimeScript™ RT reagent kit with gDNA Eraser kit (Takara Shuzo Co., Ltd., Shiga, Japan). Afterwards, cDNA was obtained from reverse transcription at 37 °C for 15 min and 85 °C for 5 s. SYBR® *Premix Ex* Taq™ (Tli RNaseH Plus) kit (Takara Co., Ltd., Shiga, Japan) was performed for RT-qPCR using a ABI7500 quantitative PCR instrument (Applied Biosystems, Foster City, CA, USA). The reaction conditions employed were as follows: pre-denaturation at 95 °C for 10 min, and 40 cycles of denaturation at 95 °C for 15 s and annealing at 60 °C for 30 s. β-actin was regarded as the internal control, while the $2^{-\Delta Ct}$ was applied to determine the ratio relationship of target gene in the observation group and the reference group. The formula applied was as follows: $\Delta\Delta CT = Ct_{\text{observation group}} - Ct_{\text{reference group}}$, in which $\Delta Ct = Ct_{\text{gene}} - Ct_{\text{β-actin}}$ [23]. Cycle threshold (Ct) was considered to be reflective of the number of amplified cycles (increased in logarithmic phase) when the real-time fluorescence intensity reached the set threshold. The primers used in the reaction are depicted in Table 1, and were procured from Shanghai GenePharma Co., Ltd. (Shanghai, China). The experiment was repeated three times.

Table 1 RT-qPCR primer sequences

Genes	Primer sequence
Ras	F: 5′-ATGACTGAATATAAACTTGT-3′
	R: 5′-TCCACAAAGTGATTCTGAAT-3′
ERK	F: 5′-GCAAGCAGCAGAGAGGAATC-3′
	R: 5′-CAAGCACAAAGCCAATCCA-3′
PPARγ	F: 5′-GTGGCTGCCTTCAACTTCTC-3′
	R: 5′-GTGGGTTGCAAACCTTCAAT-3′
HMGCS2	F: 5′-CAGCTTACCGCAGGAAAATCC-3′
	R: 5′-CAAAAGGGTGTGTGGAAGATCA-3′
β-actin	F: 5′-ACGAGGCCCAGAGCAAGA-3′
	R: 5′-TTGGTTACAATGCCGTGTTCA-3′

F forward, *R* reverse, *RT-qPCR* reverse transcription quantitative polymerase chain reaction, *PPARγ* peroxisome proliferators-activated receptor gamma, *HMGCS2* mitochondrial 3-hydroxy-3-methylglutaryl-CoA synthase 2, *ERK* extracellular signal-regulated kinase

Western blot analysis

Total protein was extracted from each CCEC rat from each group, with the protein concentration subsequently determined using a bicinchoninic acid kit (Thermo Fisher Scientific, San Jose, CA, USA). A total of 30 μg protein was electrophoresed on sodium dodecyl sulfate-polyacrylamide gel electrophoresis (SDS-PAGE) gels at 80 V for 35 min followed by 120 V for 45 min, after which, the protein was transferred onto a polyvinylidene fluoride membrane, and blocked for 1 h with 5% skimmed milk powder. After the blocking liquid was aspirated, the membrane was incubated with anti-rabbit Ras monoclonal antibody (ab52939, 1:10,000), anti-mouse ERK monoclonal antibody (ab224313, 1:2000), anti-rabbit PPARγ polyclonal antibody (ab209350, 1:500), anti-rabbit HMGCS2 monoclonal

antibody (ab137043, 1:1000) and anti-mouse β-actin monoclonal antibody (ab8225, 1:5000) at 4 °C overnight. All the aforementioned antibodies were procured from Abcam Inc. (Cambridge, MA, UK). Afterwards, the membrane was washed three times with PBS containing Tween 20 (PBST) (10 min each time). The membrane was then incubated with horseradish peroxidase-labeled secondary antibody of goat anti-rat or goat anti-rabbit (Jackson ImmunoResearch Laboratories Inc., West Grove, PA, USA) at room temperature for 1 h. Finally, the membrane was then washed three more times with PBST (10 min each time). The scanning image was obtained using optical-emission spectrometry (GE Healthcare, Chicago, Illinois, US), Image Pro Plus 6.0 software (Media Cybernetics, Inc., Silver Spring MD, USA) was used to analyze the relative protein level of protein band. The experiment was conducted three times.

Flow cytometry

The rat CCECs were collected in a tube and centrifuged at a low speed, followed by removal of the supernatant. Next, the cells were washed with cold PBS three times and centrifuged at a low speed, with the supernatant again removed. Afterwards, with cell concentration adjusted to 10^6 cells/mL, the cells were re-suspended with 500 μL binding buffer, and incubated with 5 μL Annexin-V-fluorescein isothiocyanate together with 5 μL propidium iodide (Sigma-Aldrich, St. Louis, MO, USA) under conditions void of light for 15 min. Flow cytometer was employed in order to examine cell apoptosis in each group within a 1-h period. The experiment was conducted three times.

Lactate dehydrogenase (LDH) determination

The content of LDH of rat CCECSs in nutrient solution and penis tissues was determined with an LDH kit (Nanjing Jiancheng Bioengineering Institute, Jiangsu, China). Next, the blank tube was added with 25 μL distilled water and 25 μL buffer solution, while the standard tube was added with 5 μL distilled water, 20 μL 0.2 mmol/L standard solution and 25 μL buffer solution and the test tube used to determine the LDH was added with 5 μL coenzyme I, 20 μL sample for detection and an additional 25 μL of buffer solution. The control tube was then added with 5 μL distilled water, 20 μL sample for detection and 25 μL buffer solution. After uniform mixing, the above tubes were water-bathed at 37 °C for 15 min. With the addition of 25 μL 2,4-dinitrophenylhydrazine into each tube, the above tubes were then water-bathed at 37 °C for 15 min, and then completely mixed with 250 μL NaOH solution at 0.4 mol/L. After the above tubes had been placed at room temperature for 5 min, an enzyme-linked immunosorbent assay reader (Bio-tek, Norcross, GA, USA) was employed for optical density value at the wavelength of 450 nm [24].

Statistical analysis

All data were analyzed by SPSS 21.0 (IBM Corp. Armonk, NY, USA). Results are expressed as mean ± standard deviation. Comparisons between two groups were conducted with independent sample *t* test. Comparisons among multiple groups were analyzed by one-way analysis of variance (ANOVA). The normality of data was checked with Kolmogorov−Smirnov test. Comparison among multiple groups with normal distribution was assessed using the Tukey post-hoc test of one-way ANOVA. A value of $p < 0.05$ was considered to be of statistical significance.

Results

HMGCS2 is highly differentially expressed in DMED

DMED-related chip GSE2457 was screened out from GEO, with 252 genes differentially expressed in DMED then screened out with p value < 0.05 and $|\text{LogFoldChange}| > 2$ as screening threshold. The thermal map of the top ten genes is illustrated in Fig. 2a. Compared with the normal rats, HMGCS2 was the most obvious upregulated gene among the DMED rats. The top 100 genes were then subjected to KEGG pathway enrichment analysis, the results of which are displayed in Fig. 2b. The differentially expressed genes were mainly enriched in extracellular matrix (ECM) −receptor interaction, protein digestion and absorption, PPAR signaling pathway, platelet activation, focal adhesion, PI3K-Akt signaling pathway and Amoebiasis while HMGCS2 was enriched in the PPAR signaling pathway. Taken together, the above data demonstrated that HMGCS2 was upregulated in DMED.

DMED rats show activated Ras/MAPK/PPARγ pathway and upregulation of HMGCS2 expression

Blood glucose and the weight of the rats in the control and DMED groups were initially measured. There was no significant difference detected in relation to blood glucose and weight between two groups ($p > 0.05$) (Fig. 3a), while after model establishment, the blood glucose and weight in the DMED group were higher than those in the control group. Compared with the control group, the number of penile erections was significantly increased, while the ICP and ICP/MAP exhibited reduced numbers in the DMED group ($p < 0.05$) (Fig. 3b, c). Furthermore, the ultrastructure findings observed under an electron microscope revealed that compared with the corpus cavernosum penis of rats in

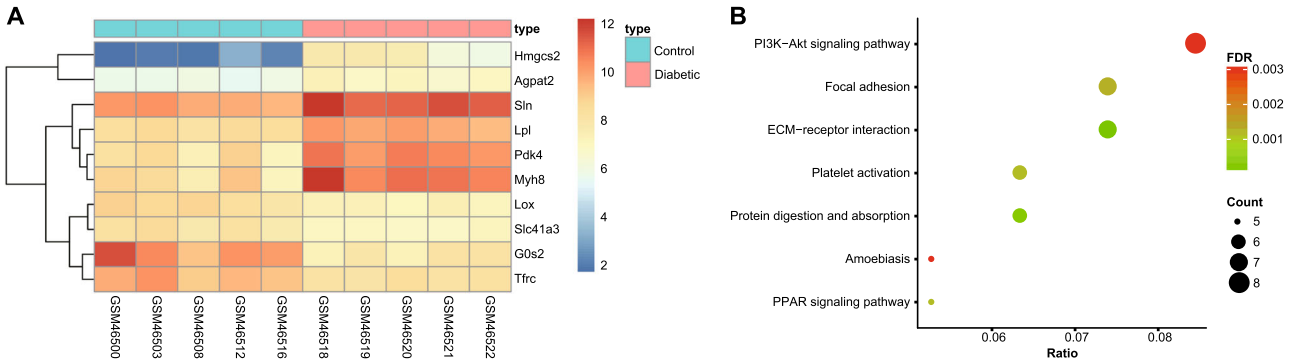

Fig. 2 HMGCS2 is obviously upregulated in DMED rats and enriched in the PPAR signaling pathway. **a** The thermal map of the first ten genes in GSE2457 chip; **b** KEGG pathway enrichment analysis. HMGCS2 Mitochondrial 3-hydroxy-3-methylglutaryl-CoA synthase 2, PPAR peroxisome proliferators-activated receptor, KEGG Kyoto Encyclopedia of Genes and Genomes, DMED diabetes mellitus-induced erectile dysfunction

the control group, the corpus cavernosum penis of rats in the DMED group exhibited broken vascular endothelium, impaired endothelial cells with abnormal forms, intravascular thrombus, in addition to impaired apoptosis of smooth muscle cells (Fig. 3d). Immunohistochemistry and RT-qPCR were conducted to identify the expression pattern of Ras, ERK, HMGCS2 and PPARγ in DMED. Results of immunohistochemistry (Fig. 3e) and RT-qPCR (Fig. 3f) displayed that compared with control group, the corpus cavernosum penis of rats in the DMED group notably elevated levels of Ras, ERK, and HMGCS2, and obviously decreased levels of PPARγ (all $p < 0.05$). The TUNEL staining (Fig. 3g) results revealed that compared with the control group, the apoptotic rate of endothelial cells was significantly increased in the DMED group ($p < 0.05$). LDH determination (Fig. 3h) revealed that the LDH level of corpus cavernosum penis in the DMED group was noticeably increased in comparison to the control group ($p < 0.05$). The results obtained implied that rats in the DMED group had impaired penile erectile function, structural impairment of the penis, obvious apoptosis and injury of endothelial cells, as well as activated Ras/MAPK/PPARγ signaling axis and upregulation of HMGCS2.

HMGCS2 silencing and inhibition of Ras/MAPK/PPARγ signaling axis ameliorate the damage in the penis

In an attempt to evaluate the Ras/MAPK/PPARγ signaling axis and HMGCS2 in DMED, an inhibitor of Ras, Simvastatin was employed to inhibit the Ras/MAPK/PPARγ signaling axis, while siRNA targeting HMGCS2 was applied to downregulate the expression of HMGCS2. Rat penile erectile function was detected and the results (Fig. 4b) indicated that compared with the siRNA-NC group, the number of penile erections was significantly increased in the Simvastatin, si-HMGCS2, and Simvastatin + si-HMGCS2 groups (all $p < 0.05$). The erectile positive rate and the number of penile erections were significantly increased in the Simvastatin + si-HMGCS2 group in comparison to the Simvastatin group ($p < 0.05$). Results of penile internal voltage detection (Fig. 4a) displayed that compared with the siRNA-NC group, the ICP and ICP/MAP were markedly elevated in the Simvastatin, si-HMGCS2, and Simvastatin + si-HMGCS2 groups (all $p < 0.05$). The ICP and ICP/MAP significantly increased in the Simvastatin + si-HMGCS2 group in comparison to the Simvastatin group ($p < 0.05$). The TEM (Fig. 4c) results revealed that rats in the siRNA-NC group exhibited broken vascular endothelium, tortuous nuclear envelope, nuclear malformation, intravascular thrombus, and shrinking and decreased number of smooth muscle cells. Rats in the Simvastatin and si-HMGCS2 groups exhibited broken and continuous vascular endothelium, swollen nuclear of endothelial cells, and impaired smooth muscle cells. Rats in the Simvastatin + si-HMGCS2 group showed well-developed endothelial cells covered with thin basement membrane that was covered with perivascular cells, and normal smooth muscle cells. The above results suggested that suppression of Ras/MAPK/PPARγ signaling axis and HMGCS2 expression level could ameliorate the structural impairment of the DMED rats' penis and reduce the rate of endothelial cell apoptosis. Moreover, the combination of inhibition of Ras/MAPK/PPARγ signaling axis and HMGCS2 silencing was determined to have exerted a greater effect on the amelioration of DMED.

HMGCS2 silencing and suppression of Ras/MAPK/PPARγ signaling axis ameliorate impairment of CCECs

To investigate the effects of Ras/MAPK/PPARγ signaling axis and HMGCS2 on the injury of CCECs in DMED rats, RT-qPCR (Fig. 5a) and immunohistochemistry (Fig. 5b)

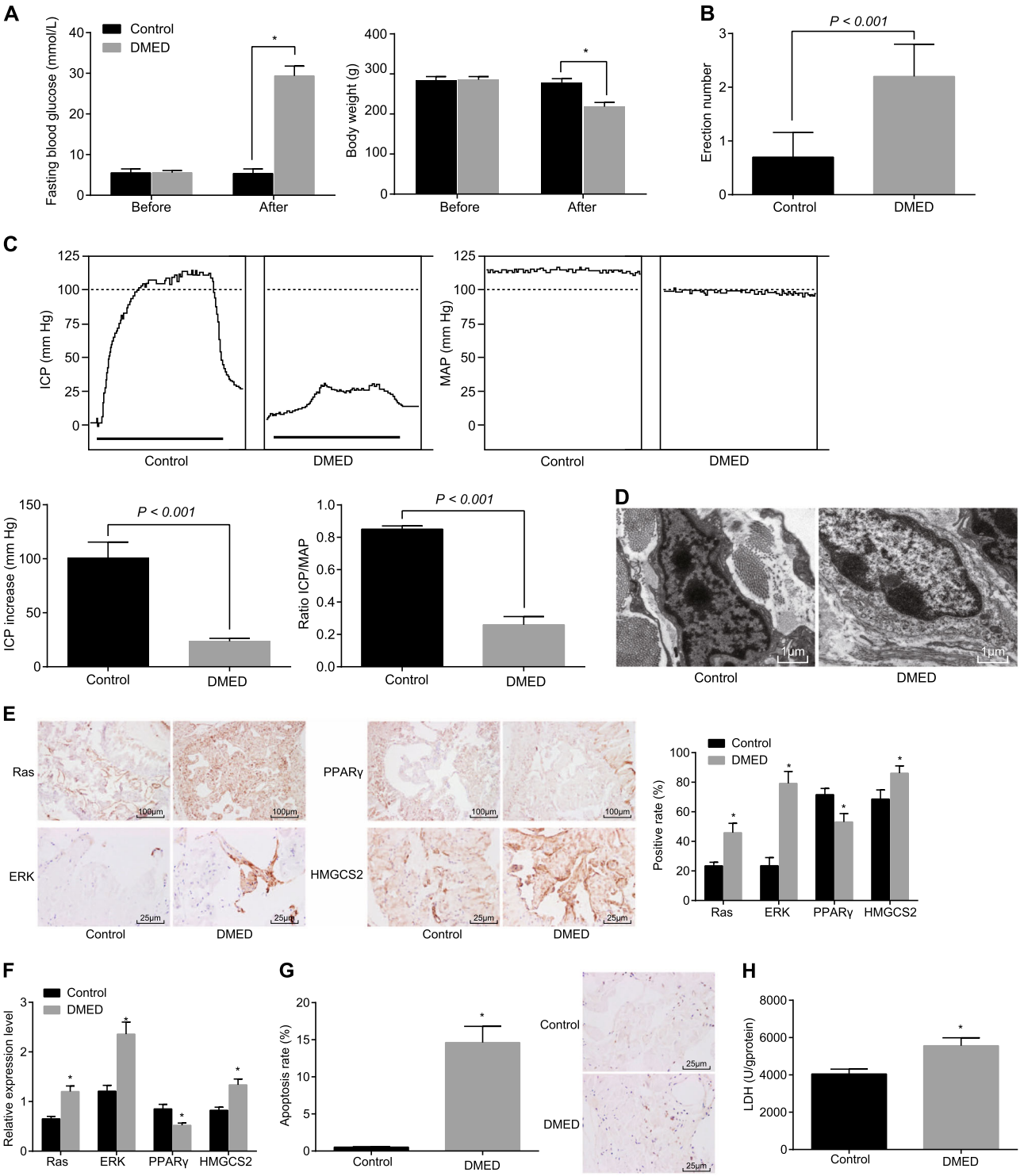

methods were adopted to determine the expression of Ras, ERK, PPARγ, and HMGCS2 in the corpus cavernosum penis of the rats. Compared with the siRNA-NC group, the Simvastatin, si-HMGCS2, and Simvastatin + si-HMGCS2 groups displayed evidently reduced levels of HMGCS2 (all $p < 0.05$). The Simvastatin + si-HMGCS2 group displayed significantly decreased levels of Ras, ERK, and HMGCS2, but elevated PPARγ level in comparison to the Simvastatin group (all $p < 0.05$). The TUNEL staining (Fig. 5c) results revealed that compared with the siRNA-NC group, the apoptotic rate of the endothelial cells was evidently reduced in the Simvastatin, si-HMGCS2, and Simvastatin + si-

◀ **Fig. 3** The corpus cavernosum tissues of rats indicate activation of the Ras/MAPK/PPARγ signaling axis, upregulated expression of HMGCS2 and impaired erectile function of the penis. **a** Blood glucose and weight of rats before and after model establishment; **b** the number of rat penile erections before and after model establishment of DMED detected by APO; **c** the ICP and ICP/MAP detected by intracavernous pressure test after model establishment of DMED; **d** ultrastructure of corpus cavernosum penis observed under TEM after model establishment of DMED (×10,000); **e** levels of Ras (×100), ERK (×400), PPARγ (×100), and HMGCS2 (×400) detected by immunohistochemistry; **f** mRNA levels of the Ras/MAPK/PPARγ signaling axis-related genes in corpus cavernosum penis tissues detected by RT-qPCR; **g** apoptotic rate of corpus cavernosum penis measured by TUNEL staining (×400); **h** LDH level of corpus cavernosum penis tissues; RT-qPCR reverse transcription quantitative polymerase chain reaction, DMED diabetes mellitus-induced erectile dysfunction, ICP intracavernous pressure, MAP mean artery pressure, APO apomorphine, TUNEL terminal deoxyribonucleotidyl transferse (TdT)-mediated biotin-16-dUTP nick-end labeling, HMGCS2 3-hydroxy-3-methylglutaryl-CoA synthase 2, PPAR peroxisome proliferators-activated receptor, TEM transmission electron microscope, LDH lactate dehydrogenase, ERK extracellular signal-regulated kinase; $*p < 0.05$ vs. the control group; the blood glucose, weight, ICP, ICP/MAP, mRNA and protein levels and LDH level before and after model establishment were measurement data, and expressed as mean ± standard deviation; an independent sample *t* test was used to analyze data; the times of penile erection was enumeration data, represented with the mean value of ten rats; mean ± standard deviation; the experiment was repeated three times; $n = 10$ (Control group), $n = 10$ (DMED group)

HMGCS2 groups (all $p < 0.05$). The Simvastatin + si-HMGCS2 group displayed a significantly decreased apoptotic rate of the endothelial cells in comparison to the Simvastatin group ($p < 0.05$). Results of LDH determination (Fig. 5d) demonstrated that compared with the siRNA-NC group, the LDH level of the corpus cavernosum penis was significantly decreased in the Simvastatin, si-HMGCS2, and Simvastatin + si-HMGCS2 groups (all $p < 0.05$). The Simvastatin + si-HMGCS2 group displayed significantly decreased LDH corpus cavernosum penis levels when compared to the Simvastatin group ($p < 0.05$). Taken together, the results obtained indicated that suppression of the Ras/MAPK/PPARγ signaling axis ameliorates the internal structure of the penis and attenuates the apoptosis of the endothelial cells by downregulating the HMGCS2 expression level. Moreover, the combination of Ras/MAPK/PPARγ signaling axis inhibition and HMGCS2 silencing exerted more profound effects on the amelioration of structural injuries of the corpus cavernosum penis.

Inactivation of Ras/MAPK/PPARγ signaling axis downregulates HMGCS2 expression

Next, the effects of the Ras/MAPK/PPARγ signaling axis on HMGCS2 expression was investigated, whereby the rat primary CCECs were subjected to various treatments (Ras/MAPK/PPARγ inhibitors or agonists) under in vitro conditions (Table 2). RT-qPCR (Fig. 6a) and western blot analysis methods (Fig. 6b) were employed in order to determine the levels of Ras, ERK, HMGCS2, and PPARγ. The results obtained indicated that compared with the control group, the TGF-α group exhibited increased levels of Ras, ERK, and HMGCS2, but decreased PPARγ level (all $p < 0.05$), while the FTS group displayed reduced levels of Ras, ERK, and HMGCS2, but elevated levels of PPARγ (all $p < 0.05$). In comparison with the TGF-α group, the TGF-α + FR180204 group displayed reduced levels of ERK and HMGCS2, while enhanced levels of PPARγ were detected (all $p < 0.05$). No significant difference in relation to Ras was detected ($p > 0.05$). In comparison to the TGF-α group, the TGF-α + RGZ group manifested lower HMGCS2 levels and higher PPARγ level (both $p < 0.05$) with no markedly changed levels of Ras and ERK ($p > 0.05$). Compared with the FTS group, the FTS + C6-Ceramide presented increased levels of ERK and HMGCS2, while reduced PPARγ level (all $p < 0.05$), with no significant difference observed in relation to the level of Ras ($p > 0.05$); whereas the FTS + GW9662 group demonstrated promoted HMGCS2 levels, with decreased levels of PPARγ (all $p < 0.05$). No significant differences in terms of the levels of Ras and ERK were detected ($p > 0.05$). The results obtained suggested that in the Ras/MAPK/PPARγ signaling axis, Ras activation could upregulate HMGCS2 by upregulating the expression of ERK to inhibit PPARγ transcription, while Ras inhibition could downregulate HMGCS2 by downregulating ERK expression which resulted in the activation of PPARγ transcription.

Overexpression of HMGCS2 impairs CCECs

In order to determine the effects of Ras/MAPK/PPARγ signaling axis and HMGCS2 overexpression on impairment of CCECs, in vitro cultured rat primary CCECs were transfected with vectors overexpressing HMGCS2 and/or Ras inhibitor, MAPK inhibitor and PPARγ agonist (Table 3). Next, RT-qPCR (Fig. 7a) and western blot analysis (Fig. 7b) were performed to determine the impairment of CCECs caused by Ras/MAPK/PPARγ signaling axis by detecting the levels of Ras, ERK, HMGCS2, and PPARγ. Compared with the control group, the HMGCS2 vector group exhibited no significant differences in the levels of Ras, ERK, and PPARγ (all $p > 0.05$), and elevated HMGCS2 level ($p < 0.05$). Compared with the HMGCS2 vector group, the HMGCS2 vector + FTS group presented that levels of Ras, ERK, and HMGCS2 were significantly reduced, while the levels of PPARγ were obviously increased (all $p < 0.05$). Compared to the HMGCS2 vector group, the HMGCS2 vector + FR180204 group displayed markedly decreased levels of ERK and HMGCS2, while significantly increased levels of PPARγ were noted (all $p < 0.05$), with no

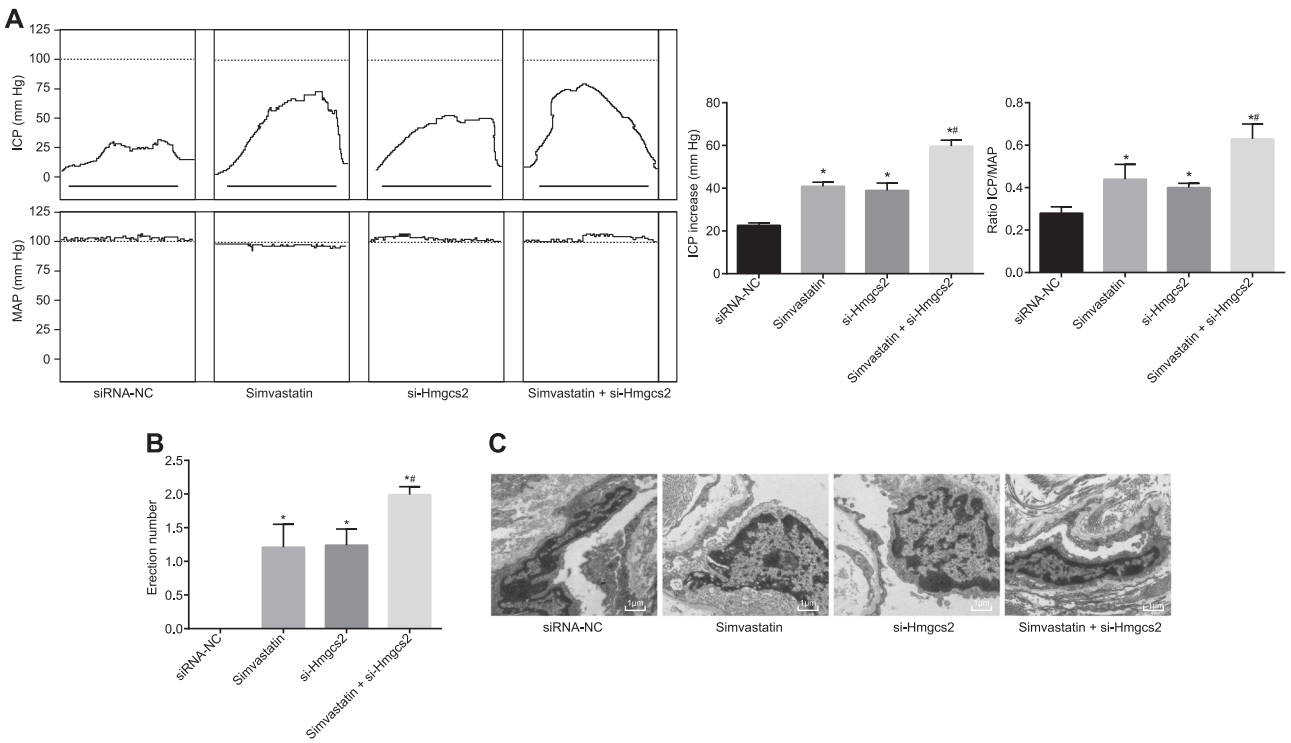

Fig. 4 HMGCS2 silencing increases the number of penile erections, ICP, and ICP/MAP, and ameliorates structure of corpus cavernosum penis. **a** The ICP and ICP/MAP values after HMGCS2 silencing and administration of Simvastatin in rats with DMED; **b** the number of penile erection after HMGCS2 silencing and administration of Simvastatin in rats with DMED measured by APO; **c** ultrastructure of corpus cavernosum penis among four groups observed under TEM (×10,000); HMGCS2 3-hydroxy-3-methylglutaryl-CoA synthase 2, TEM transmission electron microscope, ICP intracavernous pressure, MAP mean artery pressure, APO apomorphine, DMED diabetes mellitus-induced erectile dysfunction; $^{*}p < 0.05$, compared with the siRNA-NC group; $^{\#}p < 0.05$, compared with the Simvastatin group; the ICP and ICP/MAP of rats were measurement data, and expressed as mean ± standard deviation; the number of penile erection was enumeration data, represented by the mean value of eight rats; mean ± standard deviation; the one-way ANOVA was performed in order to analyze data in each group; the experiment was independently repeated three times; $n = 8$; ANOVA analysis of variance

significance difference observed in relation to the Ras levels ($p > 0.05$). In comparison with the HMGCS2 vector group, the HMGCS2 vector + RGZ group displayed notably decreased HMGCS2 levels, while the levels of PPARγ were significantly increased (all $p < 0.05$). No significant difference was detected in terms of the Ras and ERK levels (both $p > 0.05$).

Flow cytometry was performed to detect apoptosis of CCECs (Fig. 7c, d). Compared with the control group, apoptotic rate of the CCECs was obviously increased in the HMGCS2 vector group ($p < 0.05$). The apoptotic rate of CCECs was markedly decreased in the HMGCS2 vector + FTS, HMGCS2 vector + FR180204, and HMGCS2 vector + RGZ groups in comparison to the HMGCS2 vector group (all $p < 0.05$). Besides, the LDH level in the cell supernatant was detected, the results of which (Fig. 7e) demonstrated that compared with the control group, the HMGCS2 vector group exhibited an elevated LDH level of CCECs ($p < 0.05$). The LDH level of CCECs was evidently decreased in the HMGCS2 vector + FTS, HMGCS2 vector + FR180204, and HMGCS2 vector + RGZ groups in comparison to the HMGCS2 vector group (all $p < 0.05$).

A key finding of our study indicated that HMGCS2 overexpression in CCECs results in elevated levels of apoptosis of CCECs and increased LDH levels, which suggested that the growth and metabolization of endothelial cells were impaired. However, the application of Ras and MAPK inhibitors and PPARγ agonist could repair the CCECs injury caused by HMGCS2 overexpression.

HMGCS2 gene silencing attenuates impairment of CCECs under high glucose condition

To explore the effects of Ras/MAPK/PPARγ signaling axis and HMGCS2 silencing on impairment of CCECs, primary CCECs were separated from rats, and then treated with high glucose in addition to delivery of Ras agonist, MAPK agonist, PPARγ inhibitor and/or siRNA targeting HMGCS2 (Table 4) [25]. Next, RT-qPCR (Fig. 8a) and western blot analysis (Fig. 8b) were performed to determine the impairment of CCECs caused by Ras/MAPK/PPARγ signaling axis by detecting the expression levels of Ras, ERK, HMGCS2, and PPARγ. Compared with the NC group, levels of Ras, ERK, and HMGCS2 showed obvious

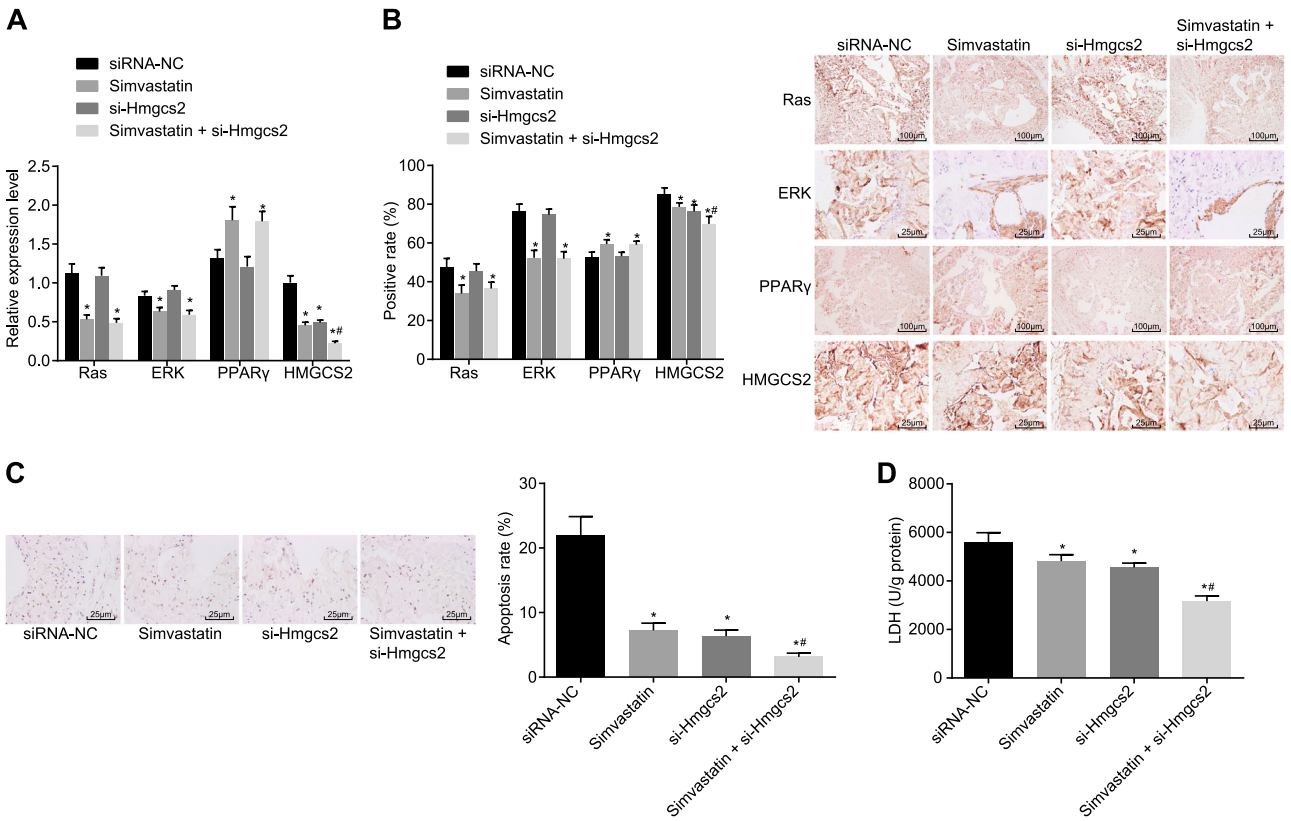

Fig. 5 HMGCS2 silencing increases PPARγ level and decrease levels of Ras, ERK, and HMGCS2, apoptosis, and LDH level in corpus cavernosum penis of DMED rats. **a** mRNA levels of Ras (×100), ERK (×400), and HMGCS2 (×400) and PPARγ (×100) in corpus cavernosum penis in DMED rats injected with Simvastatin and/or si-HMGCS2 as detected by RT-qPCR; **b protein** levels of Ras, MAPK, HMGCS2 and PPARγ in corpus cavernosum penis in DMED rats injected with Simvastatin, si-HMGCS2 or Simvastatin + si-HMGCS2 detected by immunohistochemistry; **c** apoptotic rate of CCECs in corpus cavernosum penis in DMED rats injected with Simvastatin, si-HMGCS2 or Simvastatin + si-HMGCS2 detected by TUNEL staining (×400); **d** LDH level in corpus cavernosum penis in rats injected with Simvastatin, si-HMGCS2 or Simvastatin + si-HMGCS2; RT-qPCR reverse transcription quantitative polymerase chain reaction, TUNEL terminal deoxyribonucleotidyl transferse (TdT)-mediated biotin-16-dUTP nick-end labeling, DMED diabetes mellitus-induced erectile dysfunction, CCECs corpus cavernosal endothelial cells, PPAR peroxisome proliferators-activated receptor, HMGCS2 3-hydroxy-3-methylglutaryl-CoA synthase 2, ERK extracellular signal-regulated kinase, LDH lactate dehydrogenase; $*p < 0.05$ vs. the siRNA-NC group; $\#p < 0.05$ vs. the Simvastatin group; the mRNA and protein levels of Ras, ERK, PPARγ, and HMGCS2, apoptotic rate of CCECs, and LDH level of CCECs were measurement data, and represented by mean ± standard deviation; the one-way ANOVA was performed to analyze data; the experiment was repeated three times; $n = 8$; ANOVA, analysis of variance

elevation, and PPARγ level displayed an evident reduction in the high glucose control group ($p < 0.05$). Compared with the high glucose control group, the si-HMGCS2 group showed no evident differences in relation to the levels of Ras, ERK, and PPARγ ($p > 0.05$), yet decreased HMGCS2 level ($p < 0.05$). Compared with the si-HMGCS2 group, the si-HMGCS2 + TGF-α group showed elevated levels of Ras, ERK, and HMGCS2, but decreased PPARγ level (all $p < 0.05$). Compared with the si-HMGCS2 group, the si-HMGCS2 + C6-Ceramide group displayed increased levels of ERK and HMGCS2, but reduced PPARγ level (all $p < 0.05$), with no obvious difference in relation to the level of Ras detected ($p > 0.05$). Compared with the si-HMGCS2 group, the si-HMGCS2 + GW9662 group showed decreased PPARγ level ($p < 0.05$), and no evident differences in levels of Ras, ERK, and HMGCS2 (all $p > 0.05$).

Flow cytometry was subsequently performed in order to detect the apoptosis of CCECs (Fig. 8c, d). The apoptotic rate of CCECs was evidently increased in the high glucose control group in comparison to the NC group ($p < 0.05$). Compared with the high glucose control group, the si-HMGCS2 group showed significantly decreased apoptotic rate of CCECs ($p < 0.05$). The apoptotic rate of CCECs was evidently increased in the si-HMGCS2 + TGF-α, si-HMGCS2 + C6-Ceramide, and si-HMGCS2 + GW9662 groups in comparison to the si-HMGCS2 group (all $p < 0.05$). Besides, the LDH level in cell supernatant was detected, the results of which (Fig. 8e) indicated that compared with the NC group, the LDH level of CCECs was evidently increased in the high glucose control group ($p < 0.05$). Compared with the high glucose control group, the si-HMGCS2 group exhibited notably decreased LDH levels

Table 2 Cell grouping and treatment (1)

Groups	Treatment
Control	CCECs cells were incubated for 36 h without any drug treatment
TGF-α	CCECs cells were incubated for 48 h and then cultured with 10 μM TGF-α for another 24 h
FTS	CCECs were incubated for 24 h and then cultured with 10 ng/mL FTS for another 24 h
FTS-C6-Ceramide	CCECs were incubated with 10 ng/mL FTS for 24 h and then cultured with 50 μM C6-Ceramide for another 24 h
TGF-a + FR180204	CCECs were incubated with 10 μM TGF-α for 24 h and then cultured with 50 μM FR180204 for another 24 h
FTS + GW9662	CCECs were incubated with 10 ng/mL FTS for 24 h and then cultured with 1 μM GW9662for another 24 h
TGF-α + RGZ	CCECs were incubated with 10 μM TGF-α for 24 h and then cultured with 10 μM RGZ for another 24 h

CCECs corpus cavernosal endothelial cells, *TGF-α* transforming growth factor α, *FTS* farnesylthiosalicylic acid, *RGZ* rosiglitazone

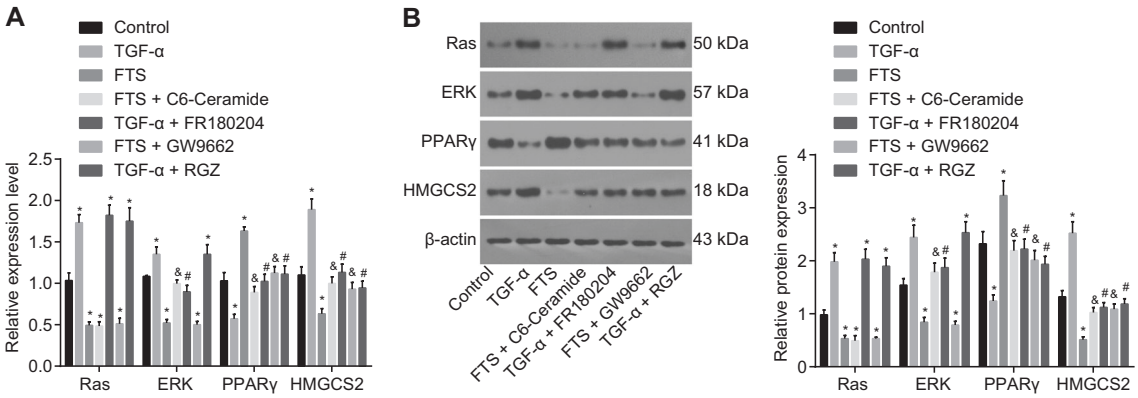

Fig. 6 Activated Ras upregulates ERK expression and downregulates PPARγ expression resulting in the upregulation of HMGCS2 expression. **a** mRNA expression of Ras, ERK, PPARγ, and HMGCS2 in CCECs, as determined by RT-qPCR; **b** protein expression of Ras, ERK, PPARγ, and HMGCS2 in CCECs, as determined by western blot analysis; RT-qPCR reverse transcription quantitative polymerase chain reaction, PPAR peroxisome proliferators-activated receptor, HMGCS2 3-hydroxy-3-methylglutaryl-CoA synthase 2, ERK extracellular signal-regulated kinase, TGF transforming growth factor, FTS farnesylthiosalicylic acid, RGZ rosiglitazone, CCECs corpus cavernosal endothelial cells; $^{*}p < 0.05$ vs. the control group; $^{\#}p < 0.05$, compared with the TGF-α group; $^{\&}p < 0.05$ vs. the FTS group; mRNA and protein levels of Ras, ERK, PPARγ, and HMGCS2 were measurement data, and represented by mean ± standard deviation; the one-way ANOVA was performed to analyze data in each group; the experiment was independently repeated three times; ANOVA analysis of variance

Table 3 Cell grouping and treatment (2)

Groups	Treatment
Control	CCECs transfected with blank plasmid and cultured for 72 h
HMGCS	CCECs transfected with HMGCS2 overexpression plasmid and cultured for 72 h
HMGCS2 vector + FTS	CCECs transfected with HMGCS2 overexpression plasmid for 48 h, and then incubated with 10 ng/mL FTS for 24 h
HMGCS2 vector + FR180204	CCECs transfected with HMGCS2 overexpression plasmid for 48 h and incubated with 50 μM FR180204 for 24 h
HMGCS2 vector + RGZ	CCECs transfected with HMGCS2 overexpression plasmid for 48 h and incubated with 10 μM RGZ for 24 h

CCECs corpus cavernosal endothelial cells, *HMGCS2* mitochondrial 3-hydroxy-3-methylglutaryl-CoA synthase 2, *FTS* farnesylthiosalicylic acid

of CCECs ($p < 0.05$). The LDH level of CCECs was markedly elevated in the si-HMGCS2 + TGF-α, si-HMGCS2 + C6-Ceramide, and si-HMGCS2 + GW9662 groups in comparison to the si-HMGCS2 group (all $p < 0.05$).

All these results indicated that high glucose environment could lead to an increased apoptosis of CCECs and higher LDH level, which suggested that CCECs were injured. However, HMGCS2 knockdown could attenuate apoptosis of CCECs and release of LDH caused by high glucose environment, while the application of Ras and MAPK agonists and PPARγ inhibitor could reverse the improved state of CCEC injury resulting from the loss of HMGCS2.

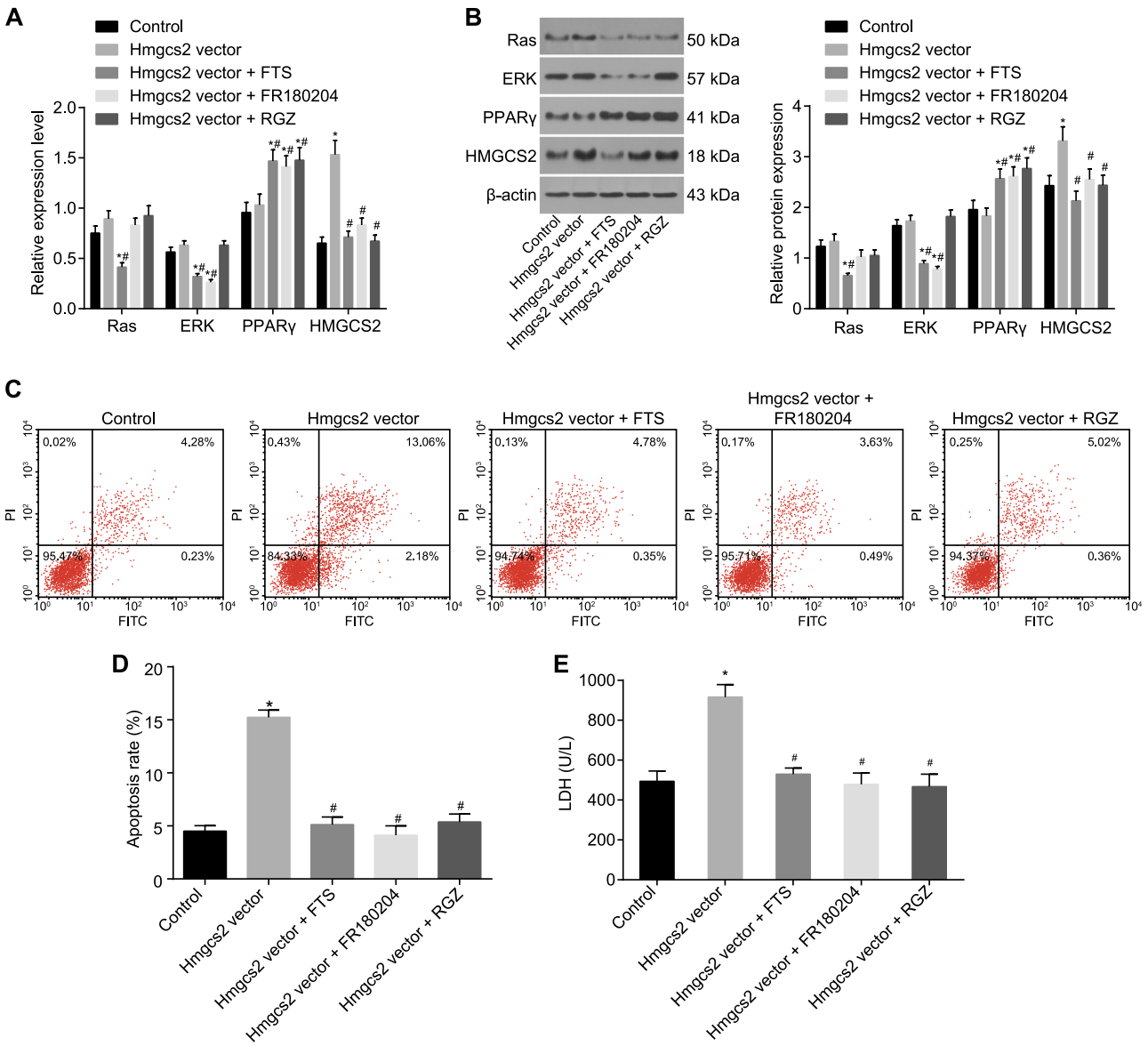

Fig. 7 HMGCS2 overexpression aggravates impairment and promotes apoptosis of CCECs by activating Ras/MAPK/PPARγ signaling axis in vitro. **a** mRNA levels of Ras, ERK, PPARγ, and HMGCS2 in CCECs after HMGCS2 overexpression as determined by RT-qPCR; **b** protein expression of Ras, ERK, PPARγ, and HMGCS2 in CCECs after HMGCS2 overexpression as determined by western blot analysis; **c** and **d** apoptotic rate of CCECs after HMGCS2 overexpression measured by flow cytometry; **e** LDH level of CCECs in cell supernatant after HMGCS2 overexpression; RT-qPCR reverse transcription quantitative polymerase chain reaction, MAPK mitogen-activated protein kinase, PPAR peroxisome proliferators-activated receptor, HMGCS2 3-hydroxy-3-methylglutaryl-CoA synthase 2, ERK extracellular signal-regulated kinase, TGF transforming growth factor, FTS arnesylthiosalicylic acid, RGZ rosiglitazone, CCECs corpus cavernosal endothelial cells, LDH lactate dehydrogenase; $^{*}p < 0.05$ vs. the control group; $^{\#}p < 0.05$ vs. the HMGCS2 vector group; mRNA and protein levels of Ras, ERK, PPARγ, and HMGCS2, apoptotic rate of CCECs, and LDH level of CCECs were measurement data, and represented by mean ± standard deviation; the one-way ANOVA was performed to analyze data in each group; the experiment was independently repeated three times; ANOVA analysis of variance

Discussion

Diabetic patients worldwide display an increased susceptibility to ED, representing a significant issue threatening male health on a global scale [26]. During the present study, through combination of in vitro experiment and in vivo experiment, we concluded that the impairment of DMED could be attenuated by suppressing the activation of the Ras/MAPK/PPARγ signaling axis and silencing HMGCS2.

Based on our in vivo experiment observations, in the successfully modeled DMED rats, the expression of Ras, ERK, and HMGCS2 was upregulated while the expression of PPARγ in the corpus cavernosum of the penis was downregulated. After the DMED rats were injected with

Table 4 Cell grouping and treatment (3)

Groups	Treatment
NC	CCECs cells transfected with NC siRNA and cultured in DMEM containing 10% FBS for 72 h
High glucose control	CCECs cells transfected with NC siRNA, and cultured in high glucose medium containing 10% FBS for 72 h
si-HMGCS2	CCECs cells transfected with HMGCS2 interfered siRNA, and cultured in high glucose medium containing 10% FBS for 72 h
si-HMGCS2 + TGF-α	CCECs cells transfected with HMGCS2 interfered siRNA for 48 h, incubated with 10 μM TGF-α for 24 h, and cultured in high glucose medium containing 10% FBS
si-HMGCS2 + C6-Ceramide	CCECs cells transfected with HMGCS2 interfered siRNA for 48 h, incubated with 50 μM C6-Ceramide for 24 h, and cultured in high glucose medium containing 10% FBS
si-HMGCS2 + GW9662	CCECs cells transfected with HMGCS2 interfered siRNA for 48 h, incubated with 1 μM GW9662 for 24 h, and cultured in high glucose medium containing 10% FBS

CCECs corpus cavernosal endothelial cells, *HMGCS2* mitochondrial 3-hydroxy-3-methylglutaryl-CoA synthase 2, *TGF-α* transforming growth factor α, *NC* negative control, *DMEM* Dulbecco's modified eagle's medium, *FBS* fetal bovine serum

Simvastatin and/or si-HMGCS2, impairment of the internal structure of the penis was noted to be alleviated in addition to reduced endothelial cell apoptosis, which suggested that inhibition of the Ras/MAPK/PPARγ pathway and knockdown of HMGCS2 could alleviate the symptoms of DMED in DMED rats. Consistent with our study, a recent study demonstrated that HMGCS2 expression was higher in rats with Type 1 DM [27]. Hyperglycemia, a condition which was diagnosed among the DMED rats in our study, has been shown to activate Ras in stellate cells and pancreatic islet [28]. MAP ERK can be activated by oxidative stress and hyperglycemia, both of which represent regulatory function in the development of DM complications [29]. Reports have highlighted a correlation between PPARγ and hyperlipidemia associated with the regulation of insulin-mediated glucose uptake and pre-adipocyte differentiation in peripheral tissues [30]. A previous report indicated that PPARγ$^{+/-}$ mice exhibited higher levels of insulin sensitivity relative to PPARγ$^{+/+}$ controls among mice placed on a high-fat diet [31]. Simvastatin belongs to a family of HMG-CoA reductase inhibitor or statins, a drug which has been reported to inhibit the expression of Ras protein [32, 33]. Profumo et al. have demonstrated that Simvastatin could help enhance endothelial cell function, reduce inflammation and insulin resistance [34]. A previous study concluded that blocking the RAS attenuated hyperglycemia-induced pancreatic inflammation and fibrosis [35]. Lin et al. opened an investigation into the downregulation of ERK and MAPK signaling axis and concluded that it could suppress cell apoptosis [36, 37]. The activation of ERK-1 has been demonstrated to promote the development of diabetic nephropathy which is often brought on by DM [38]. Moreover, the results of our study revealed that HMGCS2 silencing in connection with inhibition of the Ras/MAPK/PPARγ signaling axis was a more effective treatment approach for DMED.

The cell experiments performed provided verification that the Ras/MAPK/PPARγ signaling axis was able to downregulate the expression of HMGCS2 conferring an alleviatory effect counteracting the injuries of DMED in CCECs. DM is widely known to share an association with the apoptosis of multiple cell types, such as the cavernous smooth muscle cells [39]. A general consensus exists regarding HMGCS2 and its participation in the ketone synthesis pathways, belonging to one of the proteins in the 3-hydroxy-3-methylglutaryl-coenzyme A (HMG-CoA) family [40]. Accumulating evidence has indicated that HmG-CoA reductase inhibitor plays a significant role in human endothelial cell function [41]. Ras represents one of the most crucial elements involved in the MAPK pathway, which can be upregulated by several heterotrimeric G proteins [42]. Evidence has been presented verifying that HMGCS2 interacting with PPARα exerts significant effects on colorectal cancer [43]. NO is the primary regulator of the neuronal nitric oxide synthase (nNOS) and endothelial nitric oxide synthase (eNOS) isoforms of the corpus cavernosum, and has been revealed that its activity is decreased in the penis of human diabetic patients [44]. ERK has been reported to inhibit eNOS by phosphorylation of the enzyme in endothelial cells [29]. Su et al. concluded that HMGCS2 overexpression was related to the activation of ERK/c-Jun N-terminal kinase signaling axis in hepatocellular carcinoma [45]. Besides, a previous study suggested that lipophilic HMG-CoA reductase inhibitors may contribute to upregulation of eNOS elevating the risks associated with damage inflicted to muscle and other tissues [46].

During our in vivo experiment, following the administration of TNF-a, C6-ceramide, and RGZ which are known activators of RAS, ERK1/2, and PPARγ, respectively, and FTS, FR180204, and GW9662 which are inhibitors of RAS, ERK1/2, and PPARγ, respectively, we concluded that the activation of Ras could upregulate the ERK expression to

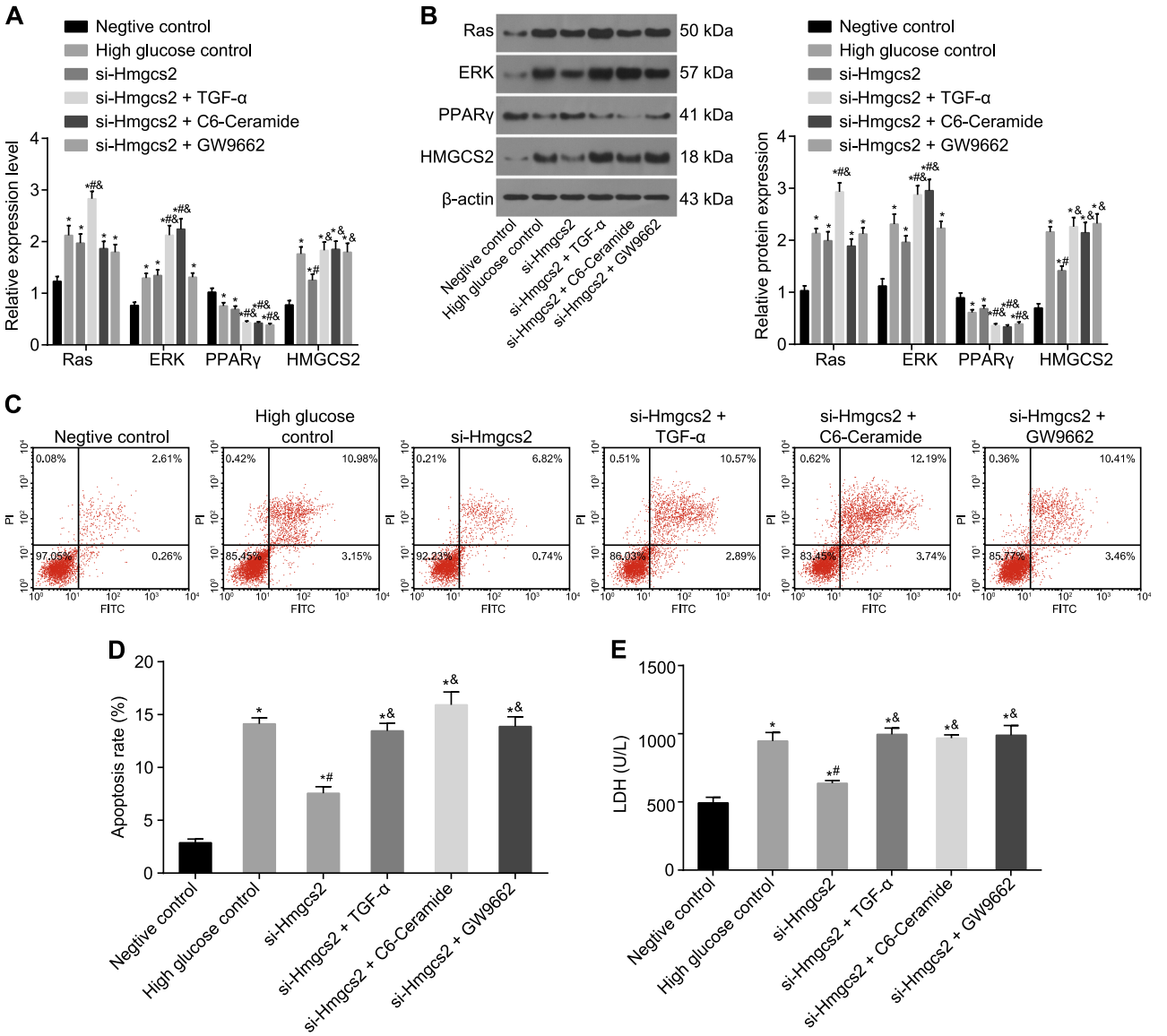

Fig. 8 HMGCS2 silencing attenuates impairment and inhibits apoptosis of CCECs under high glucose condition in vitro. **a** mRNA levels of Ras, ERK, PPARγ, and HMGCS2 in CCECs using RT-qPCR after HMGCS2 silencing; **b** protein levels and protein band patterns of Ras, ERK, PPARγ and HMGCS2 in CCECs using western blot analysis; **c** and **d** apoptotic rate of CCECs by flow cytometry under high glucose condition; **e** LDH level of CCECs in cell supernatant under high glucose condition after treatment of Ras agonist, MAPK agonist, PPARγ inhibitor and/or siRNA targeting HMGCS2; RT-qPCR reverse transcription quantitative polymerase chain reaction, MAPK mitogen-activated protein kinase, PPAR peroxisome proliferators-activated receptor, HMGCS2 3-hydroxy-3-methylglutaryl-CoA synthase 2, ERK extracellular signal-regulated kinase, TGF transforming growth factor, FTS arnesylthiosalicylic acid, RGZ rosiglitazone, CCECs corpus cavernosal endothelial cells, LDH lactate dehydrogenase; $^{*}p < 0.05$ vs. the control group; $^{\#}p < 0.05$ vs. the high glucose control group; $^{\&}p < 0.05$ vs. the si-HMGCS2 group; mRNA and protein levels of Ras, ERK, PPARγ, and HMGCS2, apoptotic rate of CCECs, and LDH level of CCECs were measurement data, and represented by mean ± standard deviation; the one-way ANOVA was performed to analyze data in each group; the experiment was repeated three times; ANOVA analysis of variance

inhibit the transcription of PPARγ, resulting in upregulated levels of HMGCS2 expression contributing to CCECs injury of DMED (Fig. 9). Taken together, based on the key observations of our study we conclude that the inactivation of Ras/MAPK/PPARγ signaling axis in connection with HMGCS2 silencing could attenuate the impairment and apoptosis of CCECs in DMED rats. Therefore, the identification of HMGCS2 silencing and Ras/MAPK/PPARγ signaling axis in DMED could help further elucidate and enhance our current understanding of the potential molecular mechanisms in DMED, highlighting their promise as novel markers for the treatment of DMED. Further studies are required in order to ascertain as to whether HMGCS2 is correlated with eNOS to fully identify and understand the specific mechanisms associated with HMGCS2 silencing on DMED via Ras/MAPK/PPARγ signaling axis.

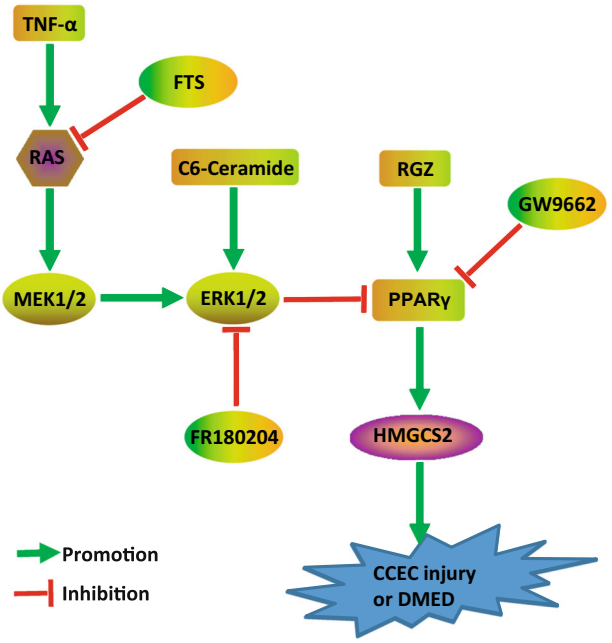

Fig. 9 Ras/MAPK/PPARγ axis regulated HMGCS2 to involve in CCEC injury of DEMD rats. Our study demonstrates that TNF-a activates Ras expression to upregulate expression of MEK1/2 and ERK1/2 so as to inhibit transcription of PPARγ; then the HMGCS2 is overexpressed, which causes CCES injury and aggravates DMEM. TNF-a, C6-ceramide, RGZ, RAS, ERK1/2 and PPARγ regulate the HMGCS2 expression through the Ras/MAPK/PPARγ signaling axis. TNF-a, C6-ceramide and RGZ are activators of RAS, ERK1/2 and PPARγ, respectively. FTS, FR180204 and GW9662 are inhibitors of RAS, ERK1/2 and PPARγ, respectively. CCECs corpus cavernosal endothelial cells, PPAR peroxisome proliferators-activated receptor, HMGCS2 3-hydroxy-3-methylglutaryl-CoA synthase 2, ERK extracellular signal-regulated kinase, TGF transforming growth factor, FTS arnesylthiosalicylic acid, RGZ rosiglitazone

Acknowledgements We would like to acknowledge the helpful comments on this paper received from our reviewers.

Compliance with ethical standards

Conflict of interest The authors declare that they have no conflict of interest.

Ethical approval This study was conducted in strict accordance with the recommendations in the Guide for the Care and Use of Laboratory Animals of the National Institutes of Health. The protocol was approved by the Institutional Animal Care and Use Committee of China-Japan Union Hospital of Jilin University.

References

1. X. Wang, C. Liu, S. Li, Y. Xu, P. Chen, Y. Liu, Q. Ding, W. Wahafu, B. Hong, M. Yang, Hypoxia precondition promotes adipose-derived mesenchymal stem cells based repair of diabetic erectile dysfunction via augmenting angiogenesis and neuroprotection. PLoS ONE **10**, e0118951 (2015)
2. R. Shamloul, H. Ghanem, Erectile dysfunction. Lancet **381**, 153–165 (2013)
3. S. Bhasin, P. Enzlin, A. Coviello, R. Basson, Sexual dysfunction in men and women with endocrine disorders. Lancet **369**, 597–611 (2007)
4. W.J. Li, M. Xu, M. Gu, D.C. Zheng, J. Guo, Z. Cai, Z. Wang, Losartan preserves erectile function by suppression of apoptosis and fibrosis of corpus cavernosum and corporal veno-occlusive dysfunction in diabetic rats. Cell. Physiol. Biochem. **42**, 333–345 (2017)
5. A. Castela, C. Costa, Molecular mechanisms associated with diabetic endothelial-erectile dysfunction. Nat. Rev. Urol. **13**, 266–274 (2016)
6. H.A. Toque, R.W. Caldwell, New approaches to the design and discovery of therapies to prevent erectile dysfunction. Expert Opin. Drug Discov. **9**, 1447–1469 (2014)
7. J. Chen, C.L. Sun, Z. Chen, H.J. Xiao, T. Qi, X.M. Li, X. Tao, B. Zhang, Separation, culture and identification of SD rat corpus cavernosal endothelial cells. Andrologia **44**, 250–255 (2012)
8. T. Rescigno, A. Capasso, M.F. Tecce, Involvement of nutrients and nutritional mediators in mitochondrial 3-hydroxy-3-methylglutaryl-CoA synthase gene expression. J. Cell. Physiol. **233**, 3306–3314 (2018)
9. J.J. Pitt, H. Peters, A. Boneh, J. Yaplito-Lee, S. Wieser, K. Hinderhofer, D. Johnson, J. Zschocke, Mitochondrial 3-hydroxy-3-methylglutaryl-CoA synthase deficiency: urinary organic acid profiles and expanded spectrum of mutations. J. Inherit. Metab. Dis. **38**, 459–466 (2015)
10. M. Shimizu, H. Moriwaki, Synergistic effects of PPARgamma ligands and retinoids in cancer treatment. PPAR Res. **2008**, 181047 (2008)
11. R.A. Hegele, Retinoid X receptor heterodimers in the metabolic syndrome. N. Engl. J. Med. **353**, 2088 (2005)
12. J. Knabl, R. Huttenbrenner, S. Hutter, M. Gunthner-Biller, T. Vrekoussis, K. Karl, K. Friese, F. Kainer, U. Jeschke, Peroxisome proliferator-activated receptor-gamma (PPARgamma) is down regulated in trophoblast cells of gestational diabetes mellitus (GDM) and in trophoblast tumour cells BeWo in vitro after stimulation with PPARgamma agonists. J. Perinat. Med. **42**, 179–187 (2014)
13. J. Li, L. Peng, H. Du, Y. Wang, B. Lu, Y. Xu, X. Ye, J. Shao, The protective effect of beraprost sodium on diabetic cardiomyopathy through the inhibition of the p38 MAPK signaling pathway in high-fat-induced SD rats. Int. J. Endocrinol. **2014**, 901437 (2014)
14. P.S. Leung, Current research of the RAS in diabetes mellitus. Adv. Exp. Med. Biol. **690**, 131–153 (2010)
15. E. Burgermeister, T. Friedrich, I. Hitkova, I. Regel, H. Einwachter, W. Zimmermann, C. Rocken, A. Perren, M.B. Wright, R. M. Schmid, R. Seger, M.P. Ebert, The Ras inhibitors caveolin-1 and docking protein 1 activate peroxisome proliferator-activated receptor gamma through spatial relocalization at helix 7 of its ligand-binding domain. Mol. Cell. Biol. **31**, 3497–3510 (2011)
16. G.K. Smyth, Linear models and empirical bayes methods for assessing differential expression in microarray experiments. Stat. Appl. Genet. Mol. Biol. **3**, Article3 (2004)
17. O. Zeng, F. Li, Y. Li, L. Li, T. Xiao, C. Chu, J. Yang, Effect of ovel gasotransmitter hydrogen sulfide on renal fibrosis and connexins expression in diabetic rats. Bioengineered **7**, 314–320 (2016)
18. C. Federau, P. Hagmann, P. Maeder, M. Muller, R. Meuli, M. Stuber, K. O'Brien, Dependence of brain intravoxel incoherent motion perfusion parameters on the cardiac cycle. PLoS ONE **8**, e72856 (2013)
19. F. Guo, X. Liu, Q. Qing, Y. Sang, C. Feng, X. Li, L. Jiang, P. Su, Y. Wang, EML4-ALK induces epithelial-mesenchymal transition consistent with cancer stem cell properties in H1299 non-small

cell lung cancer cells. Biochem. Biophys. Res. Commun. **459**, 398–404 (2015)
20. S. Renauld, K. Tremblay, S. Ait-Benichou, M. Simoneau-Roy, H. Garneau, O. Staub, A. Chraibi, Stimulation of ENaC activity by rosiglitazone is PPARgamma-dependent and correlates with SGK1 expression increase. J. Membr. Biol. **236**, 259–270 (2010)
21. M.A. Kostiuk, M.M. Corvi, B.O. Keller, G. Plummer, J.A. Prescher, M.J. Hangauer, C.R. Bertozzi, G. Rajaiah, J.R. Falck, L.G. Berthiaume, Identification of palmitoylated mitochondrial proteins using a bio-orthogonal azido-palmitate analogue. FASEB J. **22**, 721–732 (2008)
22. M. Kim, E.C. Hwang, I.K. Park, K. Park, Insulin-like growth factor-1 gene delivery may enhance the proliferation of human corpus cavernosal smooth muscle cells. Urology **76**(511), e515–e519 (2010)
23. K.J. Livak, T.D. Schmittgen, Analysis of relative gene expression data using real-time quantitative PCR and the 2(-Delta Delta C(T)) Method. Methods **25**, 402–408 (2001)
24. T. Chen, J. Zhu, C. Zhang, K. Huo, Z. Fei, X.F. Jiang, Protective effects of SKF-96365, a non-specific inhibitor of SOCE, against MPP+-induced cytotoxicity in PC12 cells: potential role of Homer1. PLoS ONE **8**, e55601 (2013)
25. H.O. Larsen, A.S. Roug, K. Nielsen, C.S. Sondergaard, P. Hokland, Nonviral transfection of leukemic primary cells and cells lines by siRNA-a direct comparison between Nucleofection and Accell delivery. Exp. Hematol. **39**, 1081–1089 (2011)
26. L. Hu, S. Qi, K. Zhang, Q. Fu, Essential role of brain-derived neurotrophic factor (bdnf) in diabetic erectile dysfunction. Andrologia **50**, (2018). 10.1111/and.12924
27. S.K. Shukla, W. Liu, K. Sikder, S. Addya, A. Sarkar, Y. Wei, K. Rafiq, HMGCS2 is a key ketogenic enzyme potentially involved in type 1 diabetes with high cardiovascular risk. Sci. Rep. **7**, 4590 (2017)
28. M. Paul, A. Poyan Mehr, R. Kreutz, Physiology of local renin-angiotensin systems. Physiol. Rev. **86**, 747–803 (2006)
29. K.P. Nunes, H.A. Toque, R.B. Caldwell, R.W. Caldwell, R.C. Webb, Extracellular signal-regulated kinase (ERK) inhibition decreases arginase activity and improves corpora cavernosal relaxation in streptozotocin (STZ)-induced diabetic mice. J. Sex. Med. **8**, 3335–3344 (2011)
30. K. Chehaibi, S. Nouira, K. Mahdouani, S. Hamdi, M. Rouis, M.N. Slimane, Effect of the PPARgamma C161T gene variant on serum lipids in ischemic stroke patients with and without type 2 diabetes mellitus. J. Mol. Neurosci. **54**, 730–738 (2014)
31. L. Chao, B. Marcus-Samuels, M.M. Mason, J. Moitra, C. Vinson, E. Arioglu, O. Gavrilova, M.L. Reitman, Adipose tissue is required for the antidiabetic, but not for the hypolipidemic, effect of thiazolidinediones. J. Clin. Invest. **106**, 1221–1228 (2000)
32. D. Falcone, L. Gallelli, A. Di Virgilio, L. Tucci, M. Scaramuzzino, R. Terracciano, G. Pelaia, R. Savino, Effects of simvastatin and rosuvastatin on RAS protein, matrix metalloproteinases and NF-kappaB in lung cancer and in normal pulmonary tissues. Cell. Prolif. **46**, 172–182 (2013)
33. N.R. Hadi, M.A. Abdelhussein, A.R. Rudha, D.A. Jamil, H.A. Al-Aubaidy, Simvastatin use in patients with type 2 diabetes mellitus: the effects on oxidative stress. Oman Med. J. **30**, 237–240 (2015)
34. E. Profumo, B. Buttari, L. Saso, R. Rigano, Pleiotropic effects of statins in atherosclerotic disease: focus on the antioxidant activity of atorvastatin. Curr. Top. Med. Chem. **14**, 2542–2551 (2014)
35. S.H. Ko, O.K. Hong, J.W. Kim, Y.B. Ahn, K.H. Song, B.Y. Cha, H.Y. Son, M.J. Kim, I.K. Jeong, K.H. Yoon, High glucose increases extracellular matrix production in pancreatic stellate cells by activating the renin-angiotensin system. J. Cell. Biochem. **98**, 343–355 (2006)
36. M.W. Lin, A.S. Lin, D.C. Wu, S.S. Wang, F.R. Chang, Y.C. Wu, Y.B. Huang, Euphol from Euphorbia tirucalli selectively inhibits human gastric cancer cell growth through the induction of ERK1/2-mediated apoptosis. Food Chem. Toxicol. **50**, 4333–4339 (2012)
37. K.Takebe, T.Nishiyama, S.Hayashi, S.Hashimoto, T.Fujishiro, N. Kanzaki, K.Kawakita, K.Iwasa, R.Kuroda, M.Kurosaka, Regulation of p38 MAPK phosphorylation inhibits chondrocyte apoptosis in response to heat stress or mechanical stress. Int. J. Mol. Med. **27**, 329–335 (2011).
38. T.M. Shiju, R. Rajkumar, N.G. Rajesh, P. Viswanathan, Aqueous extract of Allium sativum L bulbs offer nephroprotection by attenuating vascular endothelial growth factor and extracellular signal-regulated kinase-1 expression in diabetic rats. Indian J. Exp. Biol. **51**, 139–148 (2013)
39. H. Hirata, K. Kawamoto, N. Kikuno, T. Kawakami, K. Kawakami, S. Saini, S. Yamamura, R. Dahiya, Restoring erectile function by antioxidant therapy in diabetic rats. J. Urol. **182**, 2518–2525 (2009)
40. A. Vila-Brau, A.L. De Sousa-Coelho, C. Mayordomo, D. Haro, P. F. Marrero, Human HMGCS2 regulates mitochondrial fatty acid oxidation and FGF21 expression in HepG2 cell line. J. Biol. Chem. **286**, 20423–20430 (2011)
41. M. Brioschi, S. Lento, E. Tremoli, C. Banfi, Proteomic analysis of endothelial cell secretome: a means of studying the pleiotropic effects of Hmg-CoA reductase inhibitors. J. Proteom. **78**, 346–361 (2013)
42. N. Makdissy, K. Haddad, C. Mouawad, I. Popa, M. Younsi, P. Valet, L. Brunaud, O. Ziegler, D. Quilliot, Regulation of SREBPs by sphingomyelin in adipocytes via a Caveolin and Ras-ERK-MAPK-CREB signaling pathway. PLoS ONE **10**, e0133181 (2015)
43. S.W. Chen, C.T. Chou, C.C. Chang, Y.J. Li, S.T. Chen, I.C. Lin, S.H. Kok, S.J. Cheng, J.J. Lee, T.S. Wu, M.L. Kuo, B.R. Lin, HMGCS2 enhances invasion and metastasis via direct interaction with PPARalpha to activate Src signaling in colorectal cancer and oral cancer. Oncotarget **8**, 22460–22476 (2017)
44. S.G. Bernier, S. Haldar, T. Michel, Bradykinin-regulated interactions of the mitogen-activated protein kinase pathway with the endothelial nitric-oxide synthase. J. Biol. Chem. **275**, 30707–30715 (2000)
45. S.G. Su, M. Yang, M.F. Zhang, Q.Z. Peng, M.Y. Li, L.P. Liu, S. Y. Bao, miR-107-mediated decrease of HMGCS2 indicates poor outcomes and promotes cell migration in hepatocellular carcinoma. Int. J. Biochem. Cell. Biol. **91**, 53–59 (2017)
46. R.A. Parker, Q. Huang, B. Tesfamariam, Influence of 3-hydroxy-3-methylglutaryl-CoA (HMG-CoA) reductase inhibitors on endothelial nitric oxide synthase and the formation of oxidants in the vasculature. Atherosclerosis **169**, 19–29 (2003)